Investigation of Swirl Generating Characteristics of Helical Ports by Numerical Simulation

Y.Shimamoto, Y.Isshiki, T.Wakisaka and T.Fujimoto

Department of Mechanical Engineering
Kyoto University
Yoshida, Sakyo-ku
Kyoto 606
Japan

ABSTRACT

In multi-cylinder engines, uneven swirl ratios and volumetric efficiency at each cylinder may be induced, and such unevenness exerts an undesirable influence upon engine performance and exhaust emissions. In order to clarify the factors affecting such uneven swirl ratios, the relationship between flow behavior in intake system and swirl ratio has been investigated for helical ports using a technique of numerical gas flow analysis. The results show that the difference in the pattern of mass flow rate as a function of crank angle is a factor in inducing the uneven swirl ratios. Therefore, the effect of mass flow rate pattern must be taken into consideration in order to estimate the swirl ratios under actual engine conditions from the swirl characteristics in steady flows. The swirl generation under operating conditions is mostly influenced by the flow behavior in the vicinity of the maximum valve lift.

INTRODUCTION

It is well known that the performance and gaseous emissions of direct injection diesel engines depend on the air motion in cylinders, which supports air fuel mixing processes, and on the spray characteristics. The induction swirl is a factor in controlling the air motion in cylinders. As legislation concerning gaseous emissions gets more stringent worldwide, better control of induction swirl is required for developing high-speed direct injection diesel engines. It has been reported that the air motion in cylinders produced by the induction swirl is influenced by the intake port configurations (1-3). A great deal of research has been carried out on swirl generating capacity (4,5) and on velocity distribution around intake valves (6-9) under both steady and unsteady flow conditions.

In the actual engines which generally have multiple cylinders, uneven swirl ratios and volumetric efficiency at each cylinder may be induced due to a difference in the behavior of gas flow among intake valves, even if each cylinder has an intake port of the same configuration. Since uneven swirl ratios and charge air at each cylinder cause different characteristics of combustion among cylinders (10), such unevenness exerts an undesirable influence upon engine performance and exhaust emissions.

In this study, the relationship between flow behavior in intake system and swirl ratio has been investigated for helical ports using a technique of numerical gas flow analysis, for the purpose of clarifying the factors affecting such uneven swirl ratios at each cylinder.

METHOD OF ANALYSIS AND CALCULATION MODELS

First, the gas exchange process in the intake and exhaust systems of an actual engine is analyzed one-dimensionally under firing conditions by means of the characteristic method (11). Then, using the obtained temporal variations of pressure and velocity at the intake port entrance and also the obtained variation of cylinder pressure as boundary conditions, the unsteady gas flow in the intake port is calculated three-dimensionally with Cartesian coordinates (x, y, z). The gas flow is solved as a compressible viscous fluid using the finite volume method (12). For representing complicated wall shapes, a porosity approach is applied to the control volumes which are adjacent to walls(13).

The intake port models mainly investigated are shown in Fig. 1(a). Model HP-P is the helical port which is used in an actual diesel engine, and its control volumes for calculation are about 3100. Model HP-H4-P is made by reducing the height of the helical part of model HP-P, and its control volumes are about 2800. The valve position at the cylinder head is schematically shown in Fig. 1(b).

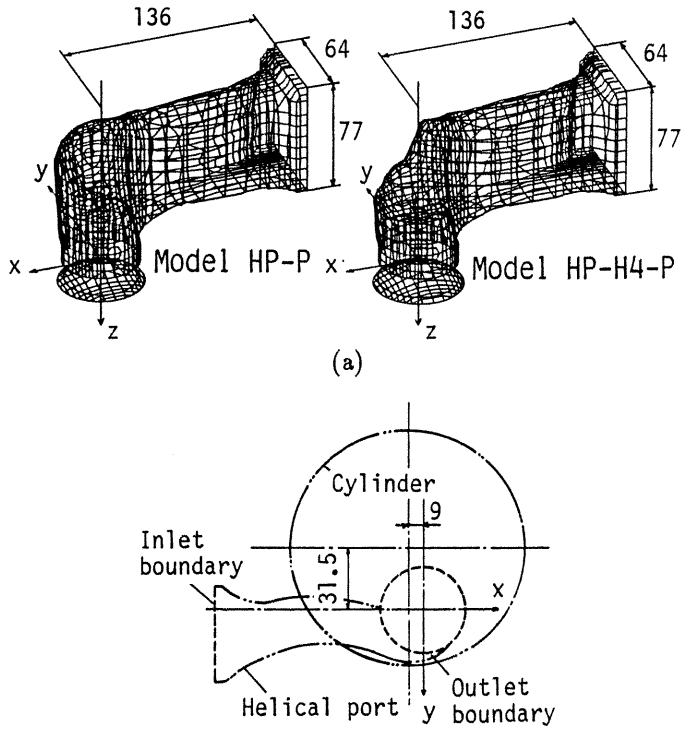

Fig. 1 Calculation models; (a) Helical port models; (b) Cylinder head

SWIRL RATIO OF A 6-CYLINDER ENGINE

The swirl ratio and volumetric efficiency have been estimated under a firing condition for an actual 6-cylinder four-cycle diesel engine. The main specifications of this engine are; bore = 108 mm, stroke = 113 mm, compression ratio = 18.9, intake valve opening = 20° BTDC, closing = 48° ABDC, and intake port diameter = 46 mm. The intake ports are similar to the helical port model HP-P shown in Fig. 1(a).

As an example, the swirl ratios S_C (see Appendix) and volumetric efficiency η_v of each cylinder at an engine speed Ne=2500 rpm are shown in Fig. 2. Since the pipe elements of the manifold have different dimensions for each cylinder due to constructional restrictions, the differences in swirl ratio and volumetric efficiency are induced among cylinders. The trend in swirl ratio for the No. 1-3 cylinder coincides with the trend in volumetric efficiency, but the trend in swirl ratio for the No. 4-6 cylinder is different from that in volumetric efficiency. Figure 3 shows the variation of mass flow rate (the mass flow per unit crank angle) m_{deg} with crank angle Θ for No. 3, 4 and 6 cylinder. It is assumed from Figs. 2 and 3 that the difference in mass flow rate pattern is a factor in inducing uneven swirl ratios at each cylinder. Accordingly, a detailed investigation of swirl generating characteristics has been performed using a single-cylinder engine.

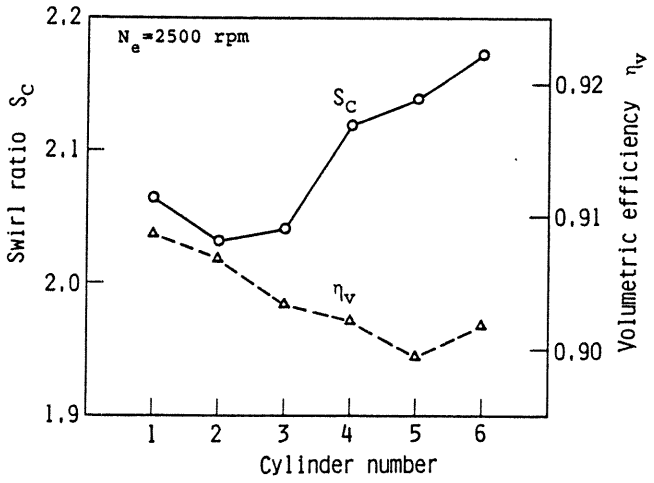

Fig. 2 Swirl ratios and volumetric efficiency at each cylinder of a 6-cylinder engine under a firing condition

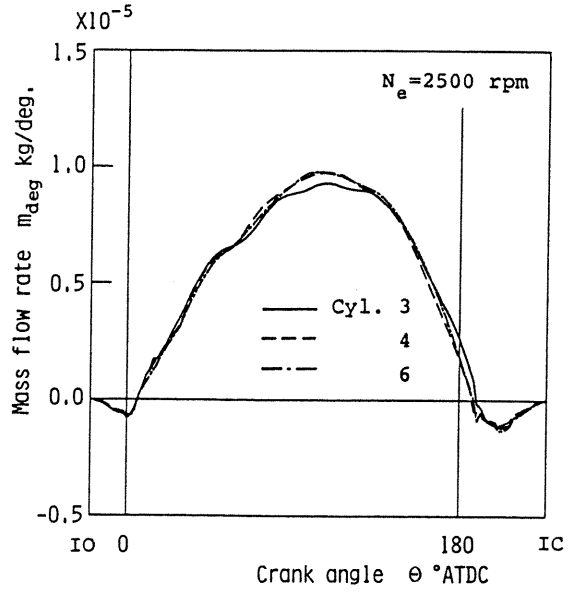

Fig. 3 Variations of mass flow rate with crank angle under a firing condition

INVESTIGATION OF SWIRL GENERATING CHARACTERISTICS USING A SINGLE-CYLINDER ENGINE

The main specifications of a single-cylinder four-cycle diesel engine investigated are; bore = 130 mm, stroke = 150 mm, compression ratio = 15.6, intake valve opening = 18° BTDC, closing = 52° ABDC, and intake port diameter = 52 mm. The two types of helical port shown in Fig. 1(a) are used for the investigation.

Investigation under Steady Flow Conditions

For models HP-P and HP-H4-P, calculations have been carried out under a steady flow condition at maximum valve lift L_v/d_v=0.275 (L_v: valve lift, d_v: port diameter); the pressure difference between the intake port entrance and the cylinder Δp=2.06 kPa.

When the velocity vector at the valve curtain area is projected on the plane perpendicular to the valve axis, it is resolved into the tangential and radial components with respect to the valve axis. The angular momentum flux Ω_C (see Appendix) with respect to the cylinder axis through the valve curtain area is resolved into three components as follows(5):

(1) Ω_{T1}: the angular momentum flux with respect to the valve axis (pre-valve component).

(2) Ω_{T2}: the angular momentum flux with respect to the cylinder axis due to the tangential component which is defined as the additional amount of momentum varied only by the eccentricity of the valve (post-valve component).

(3) Ω_R: the angular momentum flux with respect to the cylinder axis produced by the radial component due to the eccentricity of the valve (post-valve component).

The valve curtain area is divided into three equal parts which are the upper zone (U) near the valve seat, the middle zone (M) and the lower zone (L) near the valve face, as shown in Fig. 4. The angular momentum flux through each zone is also resolved into three components Ω_{T1}, Ω_{T2} and Ω_R. Figure 5 shows the components of angular momentum flux and the mass flow rate through the three zones U, M and L, and also these summations, denoted by the letter "T", respectively. It is known from the figure that the summation of angular momentum flux components of model HP-H4-P is larger than that of model HP-P by the increase in post-valve components Ω_{T2} and Ω_R, but the mass flow rate is inversely smaller because of reducing the height of helical part. The distribution ratio of three components Ω_{T1}, Ω_{T2} and Ω_R in the three zones (U, M and L) resembles each other in value. Since the distribution ratio of angular momentum flux components is considered to be a factor normalizing the profile of the velocity distribution at the valve curtain area, it is estimated that the pattern of velocity profile is not much different in the three zones.

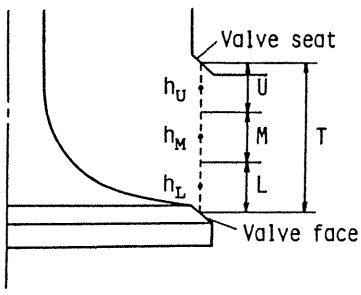

Fig. 4 Schematic diagram of the valve curtain area

The angular momentum flux through the lower zone is greater than that through the upper zone, exhibiting the same tendency in the mass flow rate. It is understood that the contribution of the angular momentum flux through the lower zone to the swirl generation is greater than that through the upper zone.

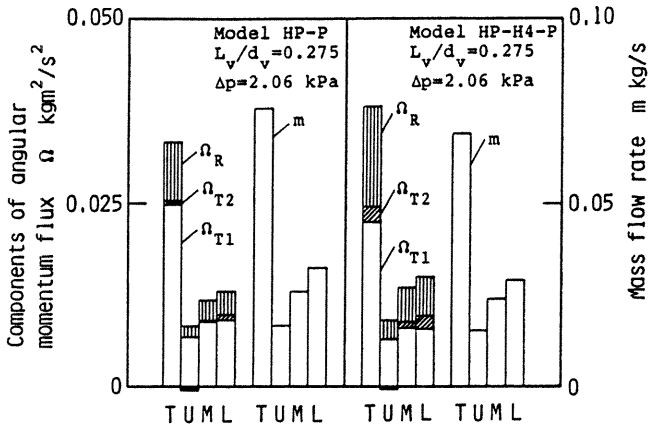

Fig. 5 Components of angular momentum flux and mass flow rate under a steady flow condition at maximum valve lift; U=upper zone, M=middle zone, L=lower zone, T=U+M+L

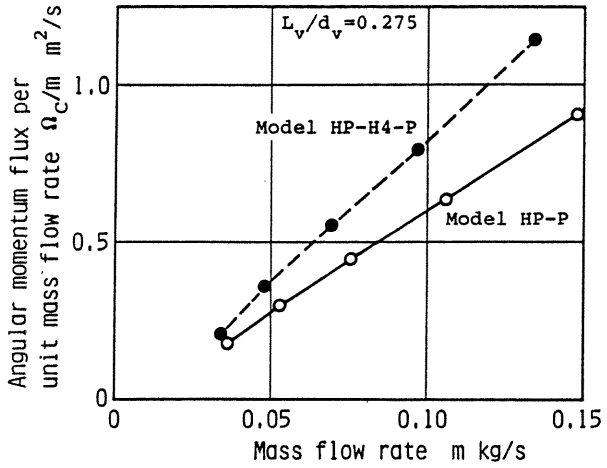

Fig. 6 Variation of angular momentum flux per unit mass flow rate with mass flow rate under steady flow conditions

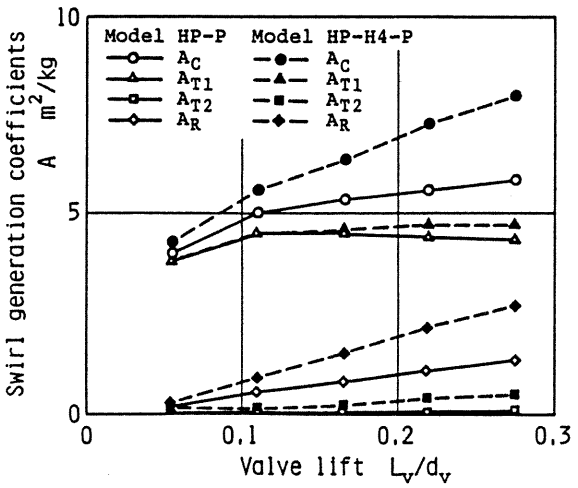

Fig. 7 Variations of swirl generation coefficients with valve lift under steady flow conditions

The variation of Ω_C/m, the angular momentum flux per unit mass flow rate through the whole valve curtain area, is shown in Fig. 6 with mass flow rate m at maximum valve lift L_v/d_v=0.275, for models HP-P and HP-H4-P respectively. The results that Ω_C/m is roughly proportional to m agree with the results obtained from impulse meter experiments(4). The angular momentum flux is considered approximately to be proportional to the square of mass flow rate under a condition of constant valve lift. Therefore, the swirl generating capacity in a steady flow may be evaluated with the proportional coefficient of Ω_C/m^2 designated as the swirl generation coefficient A. In this paper, this coefficient A is utilized for investigating the difference in swirl generating characteristics between steady and unsteady flows.

The calculations have been executed varying the valve lift L_v in conditions of roughly constant mass flow rate. The variations of swirl generation coefficients are shown in Fig. 7 with valve lift normalized by the port diameter d_v, for both models. The coefficient A_C corresponds to the angular momentum flux Ω_C, and also the coefficients A_{T1}, A_{T2} and A_R corresponds to the components of angular momentum flux Ω_{T1}, Ω_{T2} and Ω_R, respectively. Since the coefficient A_{T1} for pre-valve component shows a little variation with valve lift except for the region of low lift in both models, the angular momentum generated in the valve port is presumably not affected by the valve lift. Alternatively the coefficients A_{T2} and A_R which refer to the post-valve components are reduced with the decrease in valve lift, as the irregularity of the velocity distribution at the valve curtain area is supposedly smoothed through the valve gap. The angular momentum flux Ω_C with respect to the cylinder axis is considered to vary with valve lift owing to the smoothing effect on the post-valve components.

Investigation under Unsteady Flow Conditions

Calculations have been carried out under a motored condition at an engine speed N_e=1800 rpm with the intake port directly open to the atmosphere (the intake port length of 0.20 m). Figure 8 shows the variations of valve lift L_v, mass flow rate m_{deg}, angular momentum flux Ω_C, and contribution rates of each angular momentum flux component Ω_{T1}/Ω_C and $(\Omega_{T1}+\Omega_{T2})/\Omega_C$ with crank angle Θ, for model HP-P. Figure 9 shows the velocity distributions at three crank angles for the three sections h_U, h_M and h_L which are in the center of each zone in Fig. 4. In Fig. 8 the contribution rate Ω_{T1}/Ω_C for pre-valve component in the early and late phases of the induction period shows considerable variation as a result of the generating lag of angular momentum in the valve port. In the middle phase there is a little variation in the contribution rate. These characteristics are more clearly understood from Fig. 9. In the early phase (Θ=37° ATDC) the velocity distributions in all three zones consisted approximately of only radial velocity components, but in the middle phase (Θ=107° ATDC) tangential velocity components appear with uneven radial velocity components. At Θ=177° in the late phase tangential velocity components can be seen.

The variation of swirl generation coefficient A_C with valve lift is shown in Fig. 10 under a motored condition for models HP-P and HP-H4-P respectively. On the assumption that the mass flow rate does not vary with valve lift, the coefficient A_C of steady flow is re-plotted from Fig. 7 for reference. In steady flow, it is presumed that the influence of mass flow rate on the coefficient A_C is small and the difference in A_C between the valve opening and closing processes is not large, as the angular momentum flux per unit mass flow rate is roughly proportional to the mass flow rate in Fig. 6. Under the motored condition the large difference in A_C between both processes is caused in the region of low lift due to the swirl generating lag in the valve port. This difference in A_C becomes smaller with increasing valve lift. The velocity profile of the unsteady flow at the valve curtain area can be said to be different from that

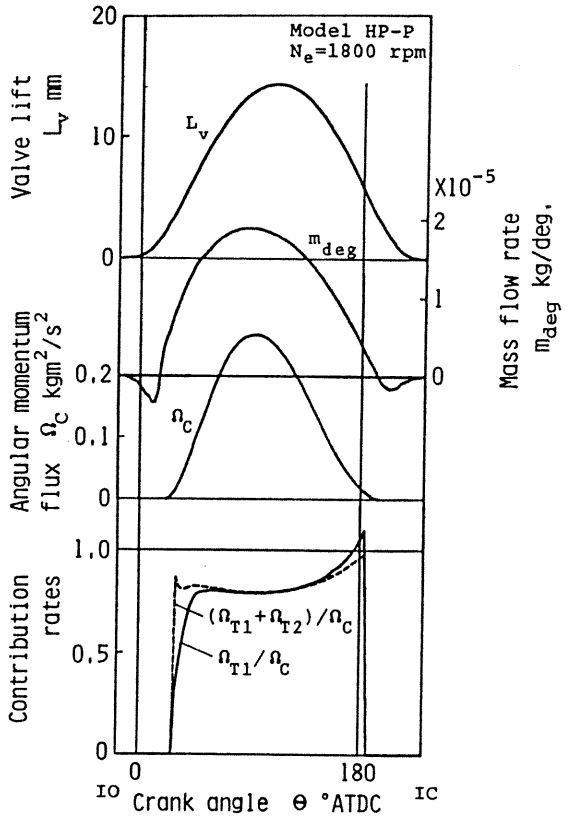

Fig. 8 Variations of valve lift, mass flow rate, angular momentum flux and contribution rates of angular momentum flux component with crank angle under a motored condition

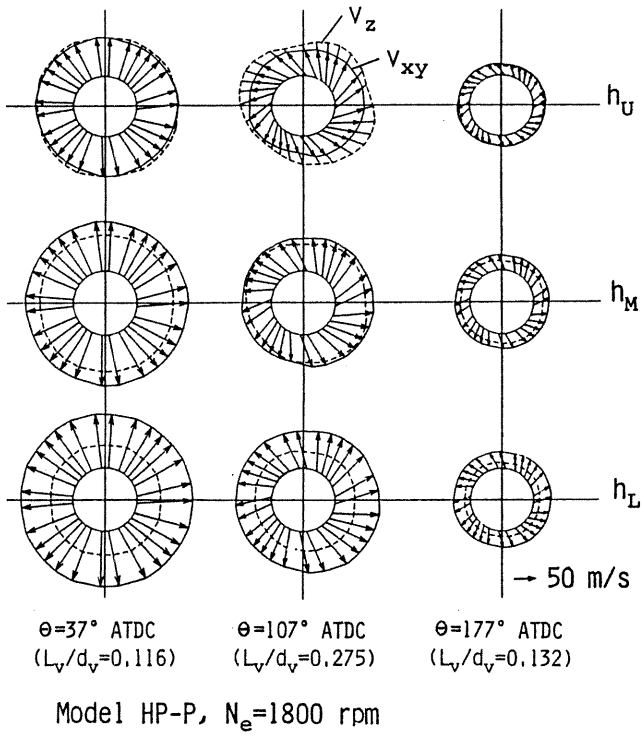

Fig. 9 Velocity distributions at the valve curtain area under a motored condition; v_{xy} = resultant velocity of radial and tangential velocity components; v_z = valve axial velocity component

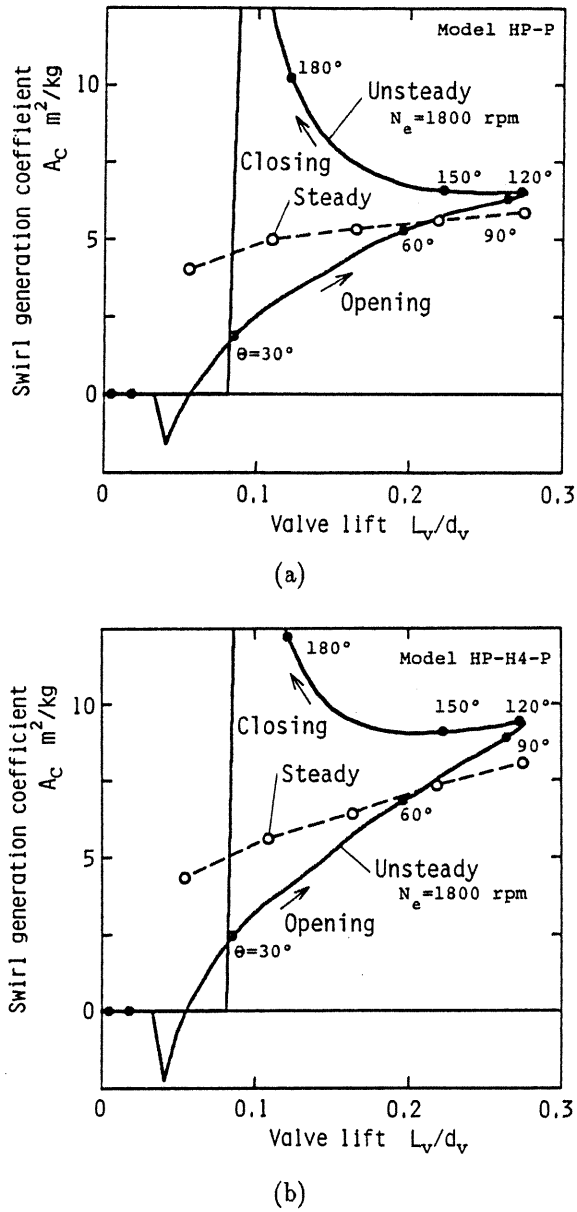

Fig. 10 Variations of swirl generation coefficient with valve lift; (a) Model HP-P; (b) Model HP-H4-P

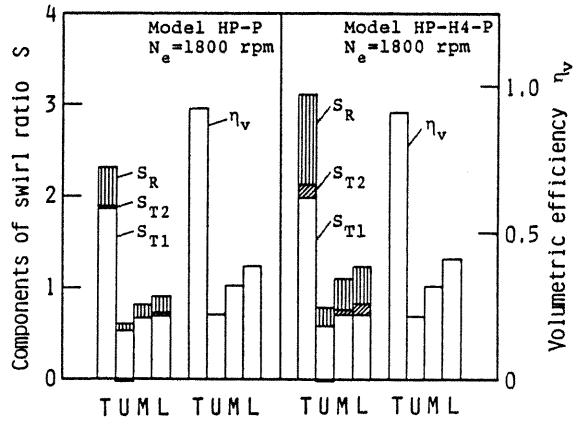

Fig. 11 Components of swirl ratio and volumetric efficiency under a motored condition; U=upper zone, M=middle zone, L=lower zone, T=U+M+L

of the steady flow in the early and late phases of the induction period, that is, at low valve lift. Alternatively the velocity profile is close to that of the steady flow in the middle phase, that is, at high valve lift.

Figure 11 shows, for models HP-P and HP-H4-P, the components of swirl ratio and the volumetric efficiency through the whole valve curtain area, designated as T, together with their values divided into three parts corresponding to the three zones U, M and L, respectively. The swirl ratio components S_{T1}, S_{T2} and S_R are the average values which are obtained by integrating the angular momentum flux components Ω_{T1}, Ω_{T2} and Ω_R through the valve curtain area for the induction period, respectively. The distribution ratio of S_{T1}, S_{T2} and S_R is closely similar to that of angular momentum flux components in Fig. 5 which is the value at the widely opened valve for the steady flow. Since the instantaneous distribution ratio of angular momentum flux components at the engine operating condition changes with the crank angle, the swirl ratio can be considered to be mainly affected by the angular momentum flux produced in the middle phase of the induction period, but to be little affected in the early and late phases.

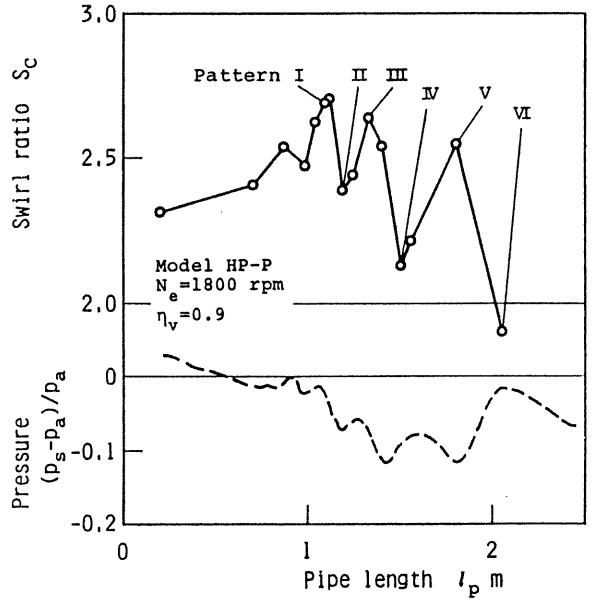

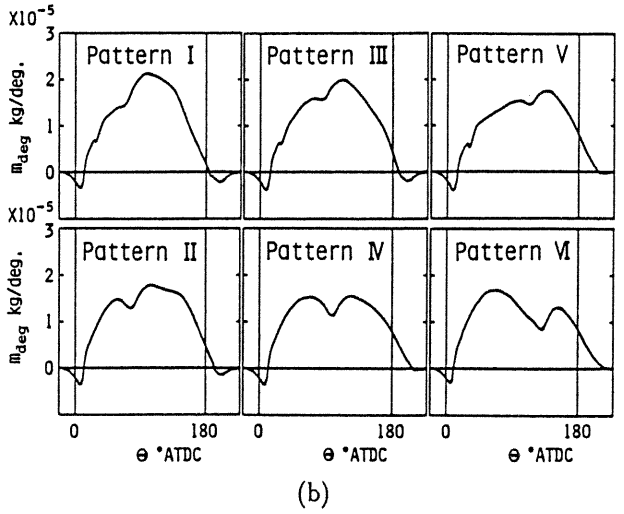

Fig. 12 Relationship between swirl ratio and mass flow rate pattern under motored conditions for model HP-P; (a) Variations of swirl ratio and pressure with intake pipe length; (b) Mass flow rate patterns

Influence of Mass Flow Rate Pattern

In order to vary the pattern of mass flow rate, an intake pipe is attached to the intake port entrance and the pressure at the pipe entrance is set at a constant value. The calculations have been carried out for model HP-P at an engine speed N_e=1800 rpm, by changing the intake pipe length l_p. In order to eliminate the effect of the volumetric efficiency on the swirl ratio, the volumetric efficiency is kept 0.9 by setting the pressure p_s at the intake pipe entrance to a suitable value. The change in swirl ratio due to the change in p_s is estimated to be less than 1.5%. Figure 12 shows the swirl ratio S_C and the patterns of mass flow rate m_{deg} for different pipe length, together with the pressure $(p_s - p_a)/p_a$ at the intake pipe entrance normalized by atmospheric pressure p_a. The patterns of the group I, III and V of high swirl ratio are obviously different from those of the group II, IV and VI of low swirl ratio. Then in the middle phase, m_{deg} of the former group is larger than m_{deg} of the latter group.

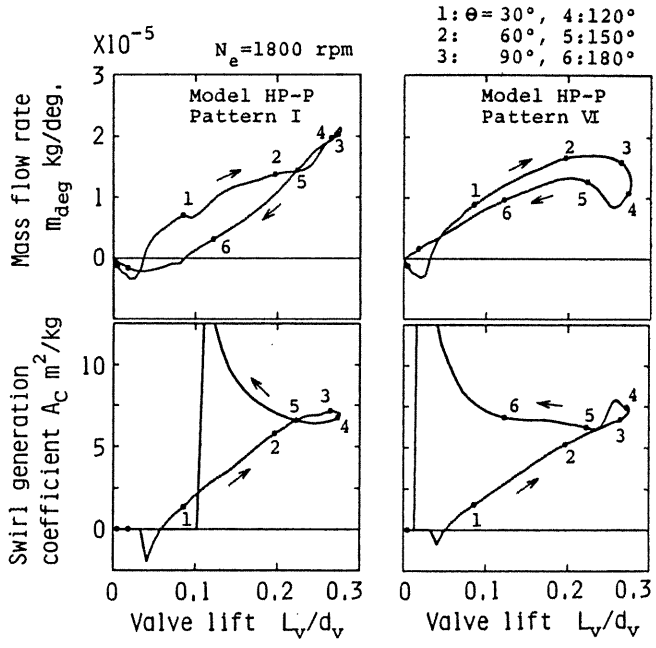

Fig. 13 Variations of mass flow rate and swirl generation coefficient with valve lift under motored conditions for model HP-P (patterns I and VI)

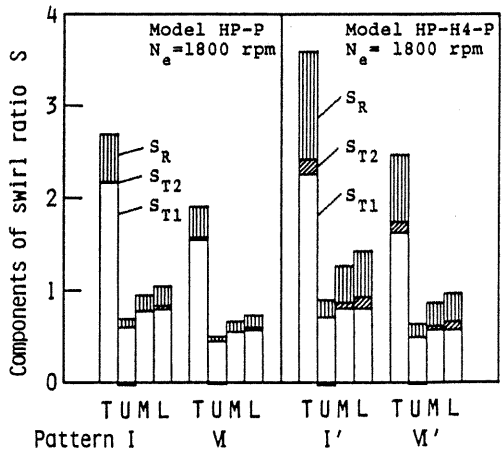

Fig. 14 Components of swirl ratio under motored conditions for models HP-P (patterns I, VI) and HP-H4-P (patterns I', VI')

For patterns I and VI, which are regarded as typical of the two groups, the mass flow rate m_{deg} and swirl generation coefficient A_C are shown in Fig. 13 as a function of valve lift. The mass flow rate of pattern I at high valve lift is larger than that of pattern VI, but the swirl generation coefficients of both patterns are not very different. Therefore the changes in swirl ratio which is caused by the difference in pattern of mass flow rate as shown in Fig 12 are a result not of the difference in A_C, that is, the velocity profile at the valve curtain area, but mainly because of the difference in mass flow rate itself at high valve lift. The pattern in which the mass flow rate becomes large in the middle phase may be suggested as a suitable pattern for making the swirl ratio high.

The components of swirl ratio through the whole valve curtain area, designated as T, are shown in Fig. 14, for patterns I and VI of model HP-P, together with their values divided into three parts corresponding to the three zones U, M and L, respectively. Also the results obtained with the model HP-H4-P are shown, by choosing pattern I' and VI' which are similar to patterns I and VI respectively. For model HP-P, the components of swirl ratio S_{T1}, S_{T2} and S_R of pattern I are larger than those of pattern VI, respectively, due to the difference in the peak position of pattern, but the difference in the distribution ratio between both patterns are not large. These trends of the effect of mass flow rate pattern on the swirl ratio can be seen for model HP-H4-P whose configuration is different from model HP-P in the helical part of the intake port. Therefore it may be considered that the swirl ratio produced with the intake port of helical type are usually affected by the mass flow rate pattern. The effect of mass flow rate pattern on swirl ratio must be taken into consideration, when the swirl ratios under actual engine conditions are estimated from the swirl characteristics in steady flow. The swirl ratio may be affected considerably by the mass flow rate in the middle phase of the induction period.

CONCLUSIONS

In order to identify the factors influencing differences in swirl among cylinders, the relationship between flow behavior in intake system and swirl ratio has been investigated for helical ports. The following conclusions are obtained:

(1) When the instantaneous velocity profile at the engine operating condition is compared with that of steady flow at the same values of valve lift and mass flow rate, the instantaneous velocity profile is considerably different from the velocity profile of steady flow in the early and late phases of the induction period, that is, at low valve lift. But the difference in both patterns is small in the middle phase, that is, at high valve lift.

(2) The swirl ratio is mainly affected by the angular momentum flux produced in the middle phase of the induction period, being little affected in the early and late phases. The changes in swirl ratio due to the mass flow rate pattern may be a result mainly of the difference in mass flow rate itself at high valve lift.

(3) The difference in mass flow rate pattern is a factor which gives rise to uneven swirl ratios at each cylinder.

(4) The unsteady behavior of mass flow rate must be taken into consideration in order to estimate the swirl ratios in actual engine conditions from the swirl characteristics in steady flows.

ACKNOWLEDGMENT

This work has been supported by the Scientific Research of a Grant-in-Aid from the Ministry of Education of Japanese Government. The calculations were carried out using a FACOM M780/30 at Kyoto University Data Processing Center.

REFERENCES

1. Brandl, F., Reverencic, I., Cartellieri, W. and Dent, J.C., "Turbulent Air Flow in the Combustion Bowl of a D.I. Diesel Engine and its Effect on Engine Performance," SAE Paper No. 790040, 1979.
2. Monaghan, M.L. and Pettifer, H.F., "Air Motion and its Effect on Diesel Performance and Emissions," SAE Paper No. 810255.
3. Tindal, M.J., Williams, T.J. and Aldoory, M., "The Effect of Inlet Port Design on Cylinder Gas Motion in Direct Injection Diesel Engines," ASME Winter Annual Meeting, pp. 101-111, 1982.
4. Tanabe, S., Iwata, H. and Kashiwada, Y, "On Characteristics of Impulse Swirl Meter," Proc. Symp. on Diagnostics and Modeling of Combustion in Reciprocating Engines (COMODIA 85), Tokyo, pp. 267-272, 1985.
5. Arcoumanis, C. and Tanabe, S., "Swirl Generation by Helical Ports," SAE Paper No. 890790.
6. Bicen, A.F., Vafidis, C. and Whitelaw, J.H., "Steady and Unsteady Airflow Through the Intake Valve of a Reciprocating Engine," Trans. ASME, J. Fluids Engng., Vol. 107, pp. 413-420, 1985.
7. Khalighi, B., El Tahry, S.H. and Kuziak, Jr.W.R., "Measured Steady Flow Velocity Distributions Around a Valve/Seat Annulus," SAE Paper No. 860462.
8. Arcoumanis, C., Vafidis, C. and Whitelaw, J.H., "Valve and In-Cylinder Flow Generated by a Helical Port in a Production Diesel Engine," Trans. ASME, J. Fluids Engng., Vol. 109, pp. 368-375, 1987.
9. El Tahry, S.H., Khalighi, B. and Kuziak, Jr. W.R., "Unsteady-Flow Velocity Measurements Around an Intake Valve of a Reciprocating Engine," SAE Paper No. 870593.
10. Shigemori, M., Tsuruoka, S. and Shimoda, M., "Development of a Combustion System for a Light Duty D.I. Diesel Engine," SAE Paper No. 831296.
11. Shimamoto, Y., Oka, M. and Tanaka, Y., "A Research on Inertia Charging Effect of Intake System in Multi-Cylinder Engines," Bull. JSME, Vol. 21, No. 153, pp. 502-510, 1978.
12. Isshiki, Y., Shimamoto, Y. and Wakisaka, T., "Numerical Prediction of Effect of Intake Port Configurations on the Induction Swirl Intensity by Three-Dimensional Gas Flow Analysis," Proc. Symp. on Diagnostics and Modeling of Combustion in Reciprocating Engines (COMODIA 85), Tokyo, pp. 295-304, 1985.
13. Shimamoto, Y., Isshiki, Y, Wakisaka, T. and Uedera, M, "The Numerical Prediction of Gas Flow in Intake Ports of Four-Cycle Internal Combustion Engines (3rd Report)," (in Japanese) Trans. JSME (B), Vol. 55, No. 518, pp. 3246-3250, 1989.

APPENDIX

The angular momentum flux Ω_C with respect to the cylinder axis through the valve curtain area is expressed as

$$\Omega_C = \int_s \rho v_r v_{xy} r_c \, ds$$

where s: area of the valve curtain area, ρ: density, v_r: radial velocity component, v_{xy}: resultant velocity of radial and tangential velocity components, r_c: length of a perpendicular from the cylinder axis to the velocity vector v_{xy}.

Assuming that the friction due to the cylinder liner and piston surfaces is relatively small, the swirl ratio S_C can be expressed as

$$S_C = \int_{\Theta_{IO}}^{\Theta_{IC}} \frac{\pi}{180\omega_e} \Omega_C d\Theta \Big/ \frac{\omega_e}{2} R_C^2 M_{IC}$$

where Θ_{IO}: crank angle of intake valve opening, Θ_{IC}: crank angle of intake valve closing, ω_e: engine angular velocity, R_C: cylinder radius, M_{IC}: mass of the cylinder contents at Θ_{IC}.